SLAC-PUB-8714 [1]
hep-ph/y0012258
November 2000

CP asymmetry in the Higgs decay into the top pair due to the stop mixing

Fred Browning[a], Darwin Chang[b,c], and Wai-Yee Keung[a]

[a] *Physics Department, University of Illinois at Chicago, IL 60607-7059, USA*
[b] *NCTS and Physics Department, National Tsing-Hua University, Hsinchu 30043, Taiwan, R.O.C.*
[c] *Stanford Linear Accelerator Center, Stanford University, Stanford, CA 94309, USA*

Abstract

We investigate a potentially large CP violating asymmetry in the decay of a neutral scalar or pseudoscalar Higgs boson into the $t\bar{t}$ pair. The source of the CP nonconservation is the complex mixing in the stop $\tilde{t}_{L,R}$ sector. One of the interesting consequence is the different rates of the Higgs boson decays into CP conjugate polarized states.

[1] Work supported by the Department of Energy, Contract DE-AC03-76SF00515

1 Introduction

The standard model (SM) of particle interactions contains one CP violating parameter, which is a complex phase in the quark sector of the SM. This phase appearing in the quark mixing matrix of the charged current is expected to account for the observed CP violations in the K-$\overline{K}$ mixing, in the K decays, as well as in the potential CP violation in the B-$\overline{B}$ system.

However, it is generally believed that new physics beyond the SM must exists. One of the major motivations for this is to understand the seemingly unnaturalness of the Higgs mass at the electroweak scale in the SM, the so-called gauge hierarchy problem. In addition, due to the difficulties of the SM to account for the baryon asymmetry of the universe as well as to resolve the strong CP problem, it is widely accepted that new sources of CP violation are needed. The most popular extension of the SM that addresses the hierarchy problem is the supersymmetric standard model[1, 2]. The extension has many more new (super-)particles and parameters compared to the SM. With all these new parameters, there are many possible new sources for CP violation. The phenomenology of CP violation caused by these new sources is rich and diverse. The effect of these new sources of CP violation may surface in the data before any super-particle is discovered.

Even in the minimal supersymmetric standard model (MSSM), which only augments superpartners of known particles in SM, the Higgs sector contains new sources of CP violation in its couplings to super-particles. When the μ term in the Higgs superpotential and the soft-SUSY-breaking A terms are complex, the tri-boson-couplings between the Higgs bosons and the squarks can contain CP violation. In MSSM with the simplest universal soft supersymmetry breaking[3], there are two new CP violating couplings which can be defined to be the phases of μ and A terms in a convention that makes the others new couplings real. Therefore, these new sources of CP violation are generic of any supersymmetric theories. In addition, they also have been used as one of the leading sources of CP violation in a scheme to use MSSM to generate baryon number asymmetry of the Universe in electroweak phase transition [4]. Therefore, it should be important to look for collider phenomenology that can check these mechanism. For example, these complex couplings lead to a complex phase in the mixing[5] of stop states. It is the purpose of this paper to investigate one consequence of this CP violating source in colliders.

It is expected that the future colliders are able to produce CP violation signals[6, 7, 10, 9] in the sectors of heavy particles. In this article we study the CP asymmetry in the Higgs decay into top pairs because the large top or stop coupling to the Higgs particles can produce largest effect.

In MSSM, even with soft breaking terms and R symmetry breaking terms, there is no tree level mixing between the scalar and the pseudoscalar bosons. Therefore their couplings can be discussed separately. However, the scalar and the pseudoscalar bosons mix at one loop, and their effect has to be taken into account as we will show later.

2 Stop Mixing

The source of CP violation that we investigate here is due to the mixing in the stop mass matrix. We use the convention adopted in Ref.[8]. The mass matrix for the stop quarks

in the left-right basis is given as

$$\mathcal{M}_{\tilde{t}}^2 = \begin{pmatrix} m_Q^2 + m_t^2 + \Delta_{\tilde{t}_L} m_Z^2 \cos 2\beta & -m_t(\mu \cot\beta + A_t^*) \\ -m_t(\mu^* \cot\beta + A_t) & m_U^2 + m_t^2 + \Delta_{\tilde{t}_R} m_Z^2 \cos 2\beta \end{pmatrix}, \tag{1}$$

where $\Delta_{\tilde{t}_L} = \frac{1}{2} - \frac{2}{3}\sin^2\theta_W$, and $\Delta_{\tilde{t}_R} = -\frac{2}{3}\sin^2\theta_W$. The complex phase δ of the off-diagonal elements is the source of CP violation.

$$\mu^* \cot\beta + A_t = |\mu^* \cot\beta + A_t| e^{i\delta}. \tag{2}$$

The stop mass eigenstates, $\tilde{t}_1, \tilde{t}_2$, are related to the left and right stop states by an unitary mixing matrix

$$\begin{pmatrix} \tilde{t_L} \\ \tilde{t_R} \end{pmatrix} = \begin{pmatrix} 1 & 0 \\ 0 & e^{i\delta} \end{pmatrix} \begin{pmatrix} \cos\theta & \sin\theta \\ -\sin\theta & \cos\theta \end{pmatrix} \begin{pmatrix} \tilde{t_1} \\ \tilde{t_2} \end{pmatrix} = \mathbf{U} \begin{pmatrix} \tilde{t_1} \\ \tilde{t_2} \end{pmatrix} \tag{3}$$

The masses of these eigenstates are given by

$$m_{1,2}^2 = \tfrac{1}{2}(m_Q^2 + m_U^2 + 2m_t^2 + (\tfrac{1}{2} - \tfrac{4}{3}\sin^2\theta_W) m_Z^2 \cos 2\beta \mp \sqrt{R}) \ , \tag{4}$$

$$R = \left(m_Q^2 - m_U^2 + \frac{1}{2} m_Z^2 \cos 2\beta\right)^2 + 4m_t^2 |\mu \cot\beta + A_t^*|^2 \ . \tag{5}$$

Here we denote $\tilde{t}_1$ as the lighter state. The mixing angle is given as

$$\tan\theta = -\frac{[m_Q^2 - m_U^2 + \frac{1}{2}m_z^2 \cos 2\beta + \sqrt{R}]}{2m_t |\mu \cot\beta + A_t^*|}. \tag{6}$$

Strong gluino couplings to stops and tops in the left-right basis is given by

$$\mathcal{L}_{\tilde{g}} = -\sqrt{2} g_s \overline{t_R} \tilde{g} \tilde{t_R} - \sqrt{2} g_s \overline{t_L} \tilde{g} \tilde{t_L} \ . \tag{7}$$

In terms of mass eigenstates,

$$\mathcal{L}_{\tilde{g}} = -\sqrt{2} g_s \overline{t} (P_R \cos\theta - P_L \sin\theta e^{i\delta}) \tilde{t_1} \tilde{g} - \sqrt{2} g_s \overline{t} (P_R \sin\theta + P_L \cos\theta e^{i\delta}) \tilde{t_2} \tilde{g}, \tag{8}$$

where P_L is the left projection $\frac{1}{2}(1 - \gamma^5)$, and P_R is the right projection $\frac{1}{2}(1 + \gamma^5)$. We also need the stop-stop coupling to Z,

$$\mathcal{L}_Z = -\frac{g}{\cos\theta_W} \left[(\tfrac{1}{2} - \tfrac{2}{3}\sin^2\theta_W) \tilde{t}_L^\dagger \overleftrightarrow{i\partial^\mu} \tilde{t}_L - \tfrac{2}{3}\sin^2\theta_W \tilde{t}_R^\dagger \overleftrightarrow{i\partial^\mu} \tilde{t}_R \right] Z_\mu \ . \tag{9}$$

After mixing, the Lagrangian for the Z coupling in the $\tilde{t}_1$, $\tilde{t}_2$ basis is

$$\mathcal{L}_Z = -\frac{g}{\cos\theta_W} \left[\left(\tfrac{1}{2}\cos^2\theta - \tfrac{2}{3}\sin^2\theta_W\right) \tilde{t}_1^\dagger \overleftrightarrow{i\partial^\mu} \tilde{t}_1 + \left(\tfrac{1}{2}\sin^2\theta - \tfrac{2}{3}\sin^2\theta_W\right) \tilde{t}_2^\dagger \overleftrightarrow{i\partial^\mu} \tilde{t}_2 \right. \tag{10}$$

$$\left. + \tfrac{1}{4}\sin(2\theta) \left(\tilde{t}_1^\dagger \overleftrightarrow{i\partial^\mu} \tilde{t}_2 + \tilde{t}_2^\dagger \overleftrightarrow{i\partial^\mu} \tilde{t}_1 \right) \right] Z_\mu \ .$$

Note that the last term is real in this phase convention.

3 The Higgs couplings to stops

In MSSM, there is only one pseudoscalar boson., A^0. The pseudoscalar Higgs coupling to the stop squarks is given by the Lagrangian

$$\mathcal{L}_A = \left(\tilde{t}_1^\dagger \; \tilde{t}_2^\dagger\right) \mathbf{T}^A \begin{pmatrix} \tilde{t}_1 \\ \tilde{t}_2 \end{pmatrix} . A^0 \tag{11}$$

The matrix $\mathbf{T}^A$ is given as

$$\mathbf{T}^A = \frac{m_t}{v_2} \begin{pmatrix} 2\sin\theta\cos\theta\ \mathrm{Im}(\hat{A}) & -i(\cos^2\theta\hat{A}^* + \sin^2\theta\hat{A}) \\ i(\cos^2\theta\hat{A} + \sin^2\theta\hat{A}^*) & -2\sin\theta\cos\theta\ \mathrm{Im}(\hat{A}) \end{pmatrix}, \tag{12}$$

and $\hat{A}$ is defined as $\hat{A} = (A_t\cos\beta - \mu^*\sin\beta)e^{-i\delta}$. Note that the nonvanishing of T_{11}^A or T_{22}^A is a sure sign of CP violation already (similar to $K_L \to 2\pi$). However, if for some reason μ and A_t happen to have the same phase, T_{11}^A and T_{22}^A will vanish because in this very special case the phase in the stop mass matrix and that in the pseudoscalar couplings can be removed simultaneously.

The pseudoscalar Higgs coupling to the top quark is given by the following Lagrangian,

$$\mathcal{L}_A^Y = \frac{gm_t}{2m_W}\cot\beta\ \bar{t}i\gamma^5 t A^0. \tag{13}$$

The neutral scalar Higgs sector is made up two scalar eigenstates, H^0 and h^0. There masses are given as

$$m_{H,h}^2 = \tfrac{1}{2}\left[m_A^2 + m_Z^2 \pm \sqrt{(m_A^2+m_Z^2)^2 - 4m_A^2 m_Z^2\cos 2\beta}\right]. \tag{14}$$

Since in MSSM the constraint on the lightest scalar, h, is such that it is too light to decay into the top pair, we shall concentrate on the decay of the heavy Higgs boson, H, which can decay into the top pair. Our general framework can also be used for the decay of the lighter boson, h, of course, if for any reason that it should be heavy enough. The heavy Higgs coupling to the stops in the left-right basis is given as

$$\mathbf{T}_0^H = \begin{pmatrix} -\frac{gm_Z}{\cos\theta_W}\Delta_{\tilde{t}_L}\cos(\alpha+\beta) - \frac{gm_t^2\sin\alpha}{m_W\sin\beta} & \frac{gm_t}{2\sin\beta}(A_t^*\sin\alpha + \mu\cos\alpha) \\ \frac{gm_t}{2\sin\beta}(A_t\sin\alpha + \mu^*\cos\alpha) & -\frac{gm_Z}{\cos\theta_W}\Delta_{\tilde{t}_R}\cos(\alpha+\beta) - \frac{gm_t^2\sin\alpha}{m_W\sin\beta} \end{pmatrix}, \tag{15}$$

where the mixing angle α is given in Ref. [2]. This matrix must then be transformed into the stop mass eigenstates. This is accomplished by using the stop mixing matrix,

$$\mathbf{T}^H = \mathbf{U}^\dagger \mathbf{T}_0^H \mathbf{U}. \tag{16}$$

Its Yukawa coupling is

$$\mathcal{L}_H^Y = \frac{gm_t\sin\alpha}{2m_W\sin\beta}\ \bar{t}tH^0. \tag{17}$$

4 Helicity calculation of the matrix element

To get non-zero CP asymmetry in Higgs decays, in addition to CP violating couplings, it is necessary to get the absorptive parts from the decay amplitudes in order to overcome the constraint from the CPT theorem. We labeled S^I and P^I as the absorptive form factors of the Higgs or pseudo-Higgs couplings to the top quark. They begin to appear at the 1-loop level, unlike their dispersive parts S and P, which can exist at the tree level,

$$\mathcal{M} = \overline{u}(p)\left[(S+iS^I)\mathbf{1} + i(P+iP^I)\gamma^5\right]v(p') \ . \tag{18}$$

In the Weyl representation, the γ matrices are given by

$$\gamma^5 = \begin{pmatrix} -1 & 0 \\ 0 & 1 \end{pmatrix} \quad \gamma^0 = \begin{pmatrix} 0 & 1 \\ 1 & 0 \end{pmatrix}.$$

The free spinors of momenta p, p' and helicities λ, λ' are given by

$$u(p,\lambda) = \begin{pmatrix} \omega_{-\lambda}\chi_{+\lambda} \\ \omega_{+\lambda}\chi_{+\lambda} \end{pmatrix} \ , \qquad v(p',\lambda) = \begin{pmatrix} -\lambda'\omega_{+\lambda'}\chi_{-\lambda'} \\ \lambda'\omega_{-\lambda'}\chi_{-\lambda'} \end{pmatrix},$$

where the χ's are two component spinor eigenfunctions $\vec{\sigma}\cdot\hat{p}\ \chi_\lambda(p) = \lambda\ \chi_\lambda$. The $\omega_\pm$ are functions of the energy and momentum of the particles, $\omega_\pm = \sqrt{E \pm |p|}$. Notice that the helicities of $t\bar{t}$ must match $\lambda' = \lambda$ because of conservation of angular momentum. Our normalization of the spinor is $u_\lambda^\dagger u_\lambda = v_\lambda^\dagger v_\lambda = 2E$. The asymmetry between the left and right matrix elements is given by

$$\mathcal{A} = \frac{|\mathcal{M}_{LL}|^2 - |\mathcal{M}_{RR}|^2}{|\mathcal{M}_{LL}|^2 + |\mathcal{M}_{RR}|^2}. \tag{19}$$

The matrix elements are given by

$$\mathcal{M}_{LL} = \sqrt{s}[-\beta_t(S+iS^I) - i(P+iP^I)] \ , \tag{20}$$

$$\mathcal{M}_{RR} = \sqrt{s}[-\beta_t(S+iS^I) + i(P+iP^I)] \ , \tag{21}$$

with $\beta_t = (1-4m_t/s)^{\frac{1}{2}}$ and $s = m_H^2$. The asymmetry can finally be obtained using the definition from Eq. (19),

$$\mathcal{A} = \frac{2\beta_t(PS^I - P^IS)}{P^{I2} + P^2 + \beta_t^2 S^2 + \beta_t^2 S^{I2}} \ . \tag{22}$$

Since we assume the Higgs boson has definite CP parity at the tree level, the final state interactions due to exchanging gluons or gauge bosons in Ref. [6] are not able to produce this CP asymmetry at the one-loop level. However, the rich CP phases in the sector of SUSY partners, especially the gluino and the stop, can give rise to large $\mathcal{A}$. For scalar boson decay, the second term P^IS in $\mathcal{A}$ gives the leading contribution; while for pseudoscalar boson decay, the first term, PS^I is the leading contribution.

The polarization asymmetry is Eq.(22) can be translated into the lepton energy asymmetry[6, 11, 12] in the final semileptonic channel $t \to b\ell^+\nu$. The energy $E_0(\ell^+)$

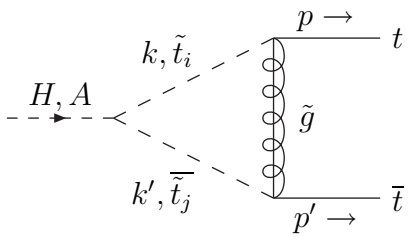

Figure 1: Triangle diagram via gluino exchange

distribution of a static t quark decay $t \to \ell^+ \nu b$ is very simple in the narrow width Γ_W approximation when m_b is negligible.

$$f(x_0) = \begin{cases} x_0(1-x_0)/D & \text{if } m_W^2/m_t^2 < x < 1, \\ 0 & \text{otherwise.} \end{cases} \tag{23}$$

Here we denote the scaling variable $x_0 = 2E_0(\ell^+)/m_t$ and the normalization factor $D = \frac{1}{6} - \frac{1}{2}(m_W/m_t)^4 + \frac{1}{3}(m_W/m_t)^6$. When the t quark is not static, but moves at a speed β_t with helicity L or R, the distribution expression becomes a convolution,

$$f_{R,L}(x, \beta_t) = \int_{x/(1+\beta_t)}^{x/(1-\beta_t)} f(x_0) \frac{\beta_t x_0 \pm (x - x_0)}{2x_0^2 \beta_t^2} dx_0 \ . \tag{24}$$

Here $x = 2E(\ell^+)/E_t$. The kernel above is related to the $(1 \pm \cos\psi)$ polar angular distribution. Similar distributions for the $\bar{t}$ decay is related by CP conjugation at the tree–level. Using the polarization asymmetry formula in Eq.(22), we can derive expressions for the energy distributions of ℓ^- and ℓ^+:

$$N^{-1} dN/dx(l^\pm) = \tfrac{1}{2}(1 \pm \mathcal{A}) f_L(x, \beta_t) + \tfrac{1}{2}(1 \mp \mathcal{A}) f_R(x, \beta_t) \ . \tag{25}$$

Here distributions are compared at the same energy for the lepton and the anti–lepton at the rest frame of the Higgs boson, $x(\ell^-) = x(\ell^+) = x = 4E(\ell^\pm)/M_H$. To prepare a large sample for analysis, we only require that each event has at least one prompt anti–lepton ℓ^+ from the t decay *or* one prompt lepton ℓ^- from the $\bar{t}$ decay.

5 Absorptive parts of 3-point vertices

We first study the triangle diagram via gluino exchange in Fig. 1..

5.1 The $\mathcal{M}_{11}$ stop loop

When the intermediate state is $\tilde{t}_1 \overline{\tilde{t}_1}$, the Feynman rule gives

$$i\mathcal{M}_{11} \ = \ (-i\sqrt{2} g_s)^2 \int \mathcal{N}_{11} \frac{i}{k^2 - m_1^2} \frac{i}{k'^2 - m_1^2} \frac{d^4 q}{(2\pi)^4} i T_{11} C_F, \tag{26}$$

where $\mathcal{N}_{11}$ is defined as

$$\mathcal{N}_{11} = \overline{u}(p)(P_R \cos\theta - P_L \sin\theta e^{i\delta}) \frac{i(\not{q} + m_{\tilde{g}})}{q^2 - m_{\tilde{g}}^2} (P_L \cos\theta - P_R \sin\theta e^{-i\delta}) v(p'). \tag{27}$$

The color factor C_F is $\frac{4}{3}$. The absorptive part of the amplitude which is needed for CP violation is obtained by cutting across the momentums k and k'. The discontinuity[13] of the matrix element is

$$\mathrm{Disc}(i\mathcal{M}_{11}) = \frac{g_s^2 T_{11}}{8\pi}\beta_1 C_F$$
$$\times \int \overline{u}(p)\frac{\not{q}(1-\gamma_5\cos 2\theta)+m_{\tilde{g}}\sin(2\theta)(-\cos\delta+i\gamma^5\sin\delta)}{q^2-m_{\tilde{g}}^2}v(p')\frac{d\Omega_k}{4\pi}\ . \tag{28}$$

The phase space integration involves the following forms,

$$J_{ij} \equiv s\int \frac{1}{q^2-m_{\tilde{g}}^2}\frac{d\,\Omega_k}{4\pi}. = \frac{1}{\beta_t\beta_{ij}}\ln\left(\frac{\beta_t^2+\beta_{ij}^2-2\beta_t\beta_{ij}+4m_{\tilde{g}}^2/s}{\beta_t^2+\beta_{ij}^2+2\beta_t\beta_{ij}+4m_{\tilde{g}}^2/s}\right), \tag{29}$$

$$s\int \frac{q^\mu}{q^2-m_{\tilde{g}}^2}\frac{d\Omega_k}{4\pi} = -H_{ij}(p-p')^\mu + K_{ij}(p+p')^\mu. \tag{30}$$

Multiplying both sides by $(p-p')_\mu$ the H_{ij} function can be isolated out because $(p+p')\cdot(p-p')$ is zero. The H_{ij} function for any intermediate mass m_i and m_j is

$$\beta_t^2 H_{ij} = 1+\tfrac{1}{4}(\beta_{ij}^2-\beta_t^2+4m_{\tilde{g}}^2/s)J_{ij}\ . \tag{31}$$

The β_{ij} function is given by

$$\beta_{ij} = \sqrt{1-2(m_i^2+m_j^2)/s+(m_i^2-m_j^2)^2/s^2}. \tag{32}$$

Notice that when $i=j$, β_{ij} reduces to $\beta_i = \sqrt{1-4m_i^2/s}$. The function K_{ij} is obtained by contracting Eq. (30) with $p+p'$.

$$K_{ij} = -\tfrac{1}{2}J_{ij}(m_i^2-m_j^2)/s\ . \tag{33}$$

Notice that for matrix elements with both the stop and the anti-stop of the same type, the term proportional to $(p+p')$ in Eq. (30) does not contribute.

After this, the imaginary part of the matrix element is needed. The imaginary parts are obtained by using the relation

$$\mathrm{Disc}(\mathcal{M}) = 2i\overline{u}(p)\left[S^I\mathbf{1}+P^I i\gamma^5\right]v(p')\ . \tag{34}$$

$$\begin{aligned} S_{11}^I &= \frac{g_s^2T_{11}\beta_1}{16\pi s}C_F\left(+m_{\tilde{g}}J_{11}\sin(2\theta)\cos\delta+2m_tH_{11}\right)\ , \\ P_{11}^I &= \frac{g_s^2T_{11}\beta_1}{16\pi s}C_F\left(-m_{\tilde{g}}J_{11}\sin(2\theta)\sin\delta\right)\ . \end{aligned} \tag{35}$$

5.2 The $\mathcal{M}_{22}$ stop loop

Similarly, we obtain results for the intermediate state $\tilde{t}_2\overline{\tilde{t}_2}$. The matrix element is given by

$$i\mathcal{M}_{22} = (-i\sqrt{2}g_s)^2\int \mathcal{N}_{22}\frac{i}{k^2-m_2^2}\frac{i}{k'^2-m_2^2}\frac{d^4q}{(2\pi)^4}iT_{22}C_F, \tag{36}$$

where $\mathcal{N}_{22}$ is given by

$$\mathcal{N}_{22} = \overline{u}(p)(P_R \sin\theta + P_L \cos\theta e^{i\delta})\frac{i(\not{q} + m_{\tilde{g}})}{q^2 - m_{\tilde{g}}^2}(P_L \sin\theta + P_R \cos\theta e^{-i\delta})v(p'). \quad (37)$$

After integrating the phase space of the intermediate state in the cut diagram, the form factors are

$$\begin{aligned} S_{22}^I &= \frac{g_s^2 T_{22}\beta_2}{16\pi s} C_F \left(-m_{\tilde{g}} J_{22} \sin(2\theta)\cos\delta + 2m_t H_{22}\right) , \quad (38) \\ P_{22}^I &= \frac{g_s^2 T_{22}\beta_2}{16\pi s} C_F \left(+m_{\tilde{g}} J_{22} \sin(2\theta)\sin\delta\right) . \end{aligned}$$

5.3 The $\mathcal{M}_{12}$ stop loop

The amplitude involving the intermediate state $\tilde{t}_1\overline{\tilde{t}_2}$ is given by

$$\begin{aligned} i\mathcal{M}_{12} &= 2i^6 g_s^2 T_{12} C_F \int \mathcal{N}_{12} \frac{1}{k^2 - m_1^2}\frac{1}{k'^2 - m_2^2}\frac{d^4q}{(2\pi)^4} \\ \mathcal{N}_{12} &= \overline{u}(p)(P_R \cos\theta - P_L \sin\theta e^{i\delta})\frac{(\not{q} + m_{\tilde{g}})}{q^2 - m_{\tilde{g}}^2}(P_L \sin\theta + P_R \cos\theta e^{-i\delta})v(p'). \quad (39) \end{aligned}$$

For $\tilde{t}_2\overline{\tilde{t}_1}$, it is

$$\begin{aligned} i\mathcal{M}_{21} &= 2i^6 g_s^2 T_{21} C_F \int \mathcal{N}_{21} \frac{1}{k^2 - m_2^2}\frac{1}{k'^2 - m_1^2}\frac{d^4q}{(2\pi)^4} , \quad (40) \\ \mathcal{N}_{21} &= \overline{u}(p)(P_R \sin\theta + P_L \cos\theta e^{i\delta})\frac{(\not{q} + m_{\tilde{g}})}{q^2 - m_{\tilde{g}}^2}(P_L \cos\theta - P_R \sin\theta e^{-i\delta})v(p') . \end{aligned}$$

After integrating over the intermediate phase space, we add up the absorptive parts to give

$$\begin{aligned} S_{12+21}^I &= -\frac{g_s^2\beta_{12}}{8\pi s} C_F \mathrm{Re}\left[m_{\tilde{g}} T_{21}(\cos^2\theta e^{i\delta} - \sin^2\theta e^{-i\delta})\right] J_{12} , \quad (41) \\ P_{12+21}^I &= -\frac{g_s^2\beta_{12}}{8\pi s} C_F \mathrm{Im}\Big[-m_{\tilde{g}} T_{21}(\sin^2\theta e^{-i\delta} + \cos^2\theta e^{i\delta}) \\ &\qquad + m_t \sin(2\theta) T_{21}(m_2^2 - m_1^2)/s\Big] J_{12} . \quad (42) \end{aligned}$$

6 Absorptive parts of 2-point vertices

We study the bubble loops which involve only the $\overline{\tilde{t}}\tilde{t}$ pair.

6.1 Z diagrams

Z diagrams that contain $\bar{\tilde{t}}_1\tilde{t}_1$ or $\bar{\tilde{t}}_2\tilde{t}_2$ are identical zero because of the phase space integration. This point will become obvious from the result of the mixed intermediate states $\tilde{t}_1\tilde{t}_2$ or $\bar{\tilde{t}}_2\tilde{t}_1$. The $\mathcal{M}_{12}$ matrix element is given below,

$$i\mathcal{M}_{12} = \frac{g^2 T_{12} N_C}{4\cos^2\theta_W}\sin(2\theta)\int \mathcal{N}_Z \frac{1}{l^2 - m_Z^2}\frac{1}{k^2 - m_1^2}\frac{1}{k'^2 - m_2^2}\frac{d^4k}{(2\pi)^4},$$

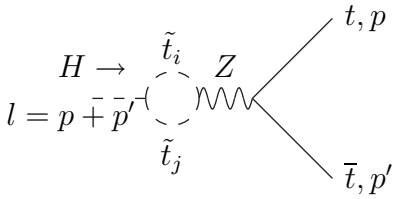

Figure 2: Z exchange diagram

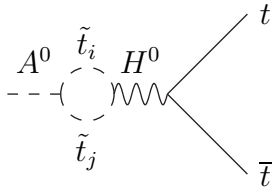

Figure 3: Higgs mixing diagram

where $\mathcal{N}_Z$ is given as

$$\mathcal{N}_Z = \overline{u}(p)\gamma^\mu \left(\tfrac{1}{4} - \tfrac{2}{3}\sin^2\theta_W - \tfrac{1}{4}\gamma^5\right) v(p') \left(g_{\mu\nu} - l_\mu l_\nu / m_Z^2\right) (k-k')_\nu \ . \tag{43}$$

The $\mathcal{M}_{21}$ matrix element is very similar to the above matrix element, with the substitution of T_{12} by T_{12}^*,

$$P^I_{12+21;Z} = \frac{g^2 N_C}{64\pi} \frac{m_t \beta_{12} \sin(2\theta)}{m_Z^2 \cos^2\theta_W} \frac{m_1^2 - m_2^2}{s} \mathrm{Im}(T_{12}) \ , \tag{44}$$

where the color factor $N_C = 3$. This graph will contribute only to CP violation of the scalar Higgs decay. One may think that without gluino couplings in the graph, one should be able to rotate away the CP violating phase in scalar coupling T_{12}^H. However, such rotation will produce a complex phase in $\tilde{t}_1^\dagger \tilde{t}_2 Z$ coupling in Eq.(10).

6.2 A^0–H^0 Mixing

The stop bubble loop induces A^0–H^0 Mixing. We study its absorptive part which contributes to the CP violation. In the heavy Higgs mass limit of MSSM, m_{A^0} and m_{H^0} are quite close to each other based on the tree-level mass relation in Eq.(14). However, it is known that there is large higher order correction to the tree-level mass relation. Thus in our following study we allow the masses m_{A^0} and m_{H^0} to vary independently, not restricted by the tree-level formula. The matrix element for the pseudoscalar Higgs turning into a stop pair, then becoming the heavy Higgs, and finally decaying into a top pair, is given as

$$i\mathcal{M} = \frac{igm_t \sin\alpha}{2m_W \sin\beta} \overline{u}(p) v(p') \sum_{ij} \int \frac{T_{ji}^{H^0}}{m_{A^0}^2 - m_H^2} \frac{T_{ij}^{A^0}}{(\frac{l}{2}+q)^2 - m_i^2} \frac{id^4q/(2\pi)^4}{(\frac{l}{2}-q)^2 - m_j^2} \ . \tag{45}$$

Making the same cut as that in the Z loop digram, we obtain the imaginary part of the form factor,

$$S^I(A^0 \to H^0 \to \bar{t}t) = -\frac{gm_t}{32\pi m_W} \frac{\sin\alpha}{\sin\beta} \sum_{ij} \beta_{ij} \frac{T_{ji}^{H^0} T_{ij}^{A^0}}{m_{A^0}^2 - m_{H^0}^2} \ . \tag{46}$$

A similar expression is derived for the heavy scalar Higgs decay,

$$P^I(H^0 \to A^0 \to \bar{t}t) = -\frac{gm_t}{32\pi m_W}\cot\beta \sum_{ij}\beta_{ij}\frac{T^{H^0}_{ji}T^{A^0}_{ij}}{m^2_{H^0}-m^2_{A^0}} \ . \tag{47}$$

7 Physical and Numerical Analyses

Before we plunge into the numerical analysis, it is interesting to check the limit in which the two stop states are accidentally degenerate. In that case, $(\mathcal{M}^2_{\tilde{t}})_{12} = (\mathcal{M}^2_{\tilde{t}})_{21} = 0$, $(\mathcal{M}^2_{\tilde{t}})_{11} = (\mathcal{M}^2_{\tilde{t}})_{22}$. Therefore $\mu^* \cot\beta + A_t = 0$, and μ^* and A_t should have the same phase which can still serve as the source of CP violation. In that case, θ and δ in $\mathbf{U}$ in Eqs.(3),(12),(16) and in the definition of $\hat{A}$, should be set to zero.

Thus in this limit, the stop loops do not contribute to $\mathcal{M}_{11}$ and $\mathcal{M}_{22}$ in the pseudoscalar case, because $T^A_{11} = T^A_{22} = 0$. However they still give rise to CP violation in $\mathcal{M}_{12}$, $\mathcal{M}_{21}$ because $T^A_{12} = (-im_t/v_2)(A^*_t\cos\beta - \mu\sin\beta)$. One may attempt to absorb this phase by rotating the phase of, say, the right stop, however such rotation will lead to complex gluino-top-stop couplings which cannot be rotated away because of the nonvanishing gluino mass. From this, it is easy to understand why a factor of gluino mass has to appear in Eq.(41) for S^I_{12+21}. Similarly, for the scalar Higgs decay in the degenerate stop limit, the stop loops still produce no CP violating effect in $\mathcal{M}_{11}$ and $\mathcal{M}_{22}$, because $\sin\theta = 0$ and only the term proportional to the gluino mass in P^I_{12+21} contributes as reflected in Eq.(42).

It is also straightforward to note that in the degenerate limit, the contributions of both H^0–Z^0 and A^0–H^0 bubble graphs vanish. In the H^0–Z^0 case, the phase of the scalar Higgs, H, coupling as well as that of the stop mixing can be rotated away simultaneously (into the gluino couplings) without affecting the Z coupling and this is reflected in $m_1^2 - m_2^2 = 0$ factor in Eq.(44). For A^0–H^0, the phase of pseudoscalar coupling as well as that of the scalar coupling can be rotated away simultaneously also and this is reflected in

$$\sum_{ij}\beta_{ij}T^{H^0}_{ji}T^{A^0}_{ij} = \beta_{12}(T^{H^0}_{21}T^{A^0}_{12} + T^{H^0}_{21}T^{A^0}_{12}) = 0 \ ,$$

in this particular limit.

To illustrate our result numerically, in the following, we set the parameters so that only the lighter stops states $\overline{\tilde{t}_1}\tilde{t}_1$ are light enough to be on-shell for simplicity. In such a scenario, only some of the above contributions are available. In Fig. 4, we show the mass m_1 of the lightest stop versus $\tan\beta$. The best current limit of the lowest bound on lightest stop mass from LEP is about 95 GeV [14], and this means that $\tan\beta < 3$ is not allowed for the case $m_Q = m_U = 300$GeV, $\mu = 500\,$GeV, $A_t = 500e^{\frac{i\pi}{4}}$ GeV. If one wishes to study the possibility of a much heavier Higgs which can decay to all channels of stops, the remaining diagrams can be easily incorporated into the numerical analysis.

7.1 Pseudoscalar-Higgs Decay

In the model of our study, the A^0 remains its status as a pseudoscalar boson at the tree level. CP violation in the pseudoscalar Higgs decay into top pairs occurs starting at the one-loop level. The leading contribution requires induced scalar form factor S^I which, as we have shown, can be obtained from the absorptive part due to the intermediate $\overline{\tilde{t}}\tilde{t}$

state. Notice that there is no Z loop contribution to S^I in the Higgs decay. Fig. 5 show the asymmetry for the pseudoscalar Higgs decay as defined by (22). Fig. 6 shows the branching ratios of the pseudoscalar-Higgs decay to top pairs, bottom pairs, and stop pairs. For small $\tan\beta$ the decay channel is mostly top pairs.

7.2 Higgs Decay

In the Higgs decay, the CP violation is caused by terms proportional to the P^I form factors. The Z diagrams can contribute in principle if not disallowed by the kinematics. As stated before it does not contribute in our illustration because we assume a heavy $\tilde{t}_2$. Fig. 7 shows the CP asymmetry of the Higgs decay. The branching ratios for the Higgs to decay into tops, bottoms, stops, W's, and Z's are given in Fig. 8.

8 Conclusion

The complex mixing among the stop sector can produce CP asymmetry at the level of a few percent in the final products of polarized $t\bar{t}$ states from the Higgs boson decay. Such asymmetry can be measured in the energy spectra of the final leptons. Unlike the usual two-Higgs-doublet model, the CP violation does not require the mixing among A^0 and H^0 states at the tree level.

This work was supported in parts by National Science Council of R.O.C., and by U.S. Department of Energy (Grant No. DE-FG02-84ER40173).

References

[1] H.P. Nilles, Phys. Rept. **110**, 1 (1984);
H. Haber and G. Kane, Phys. Rept. **117**, 75 (1985);
S. Dawson, hep-ph/9612229;
M. Drees, hep-ph/9611409;
M. Peskin, hep-ph/9705479; etc.

[2] J. Gunion, H. Haber, G. Kane, and S. Dawson, The Higgs Hunter's Guide, published by Addision-Wesley, New York (1990),

[3] For a recent review, see A. Masiero and L. Silvestrini, hep-ph/9711401 and references there-in.

[4] For a recent review, see J. M. Cline, M. Joyce and K. Kainulainen, hep-ph/0006119 and references there-in.

[5] P. Apostolos, Phys. Rev. Lett. **77** 4996, (1996).

[6] D. Chang and W.-Y. Keung, Phys. Lett. **B305**, 261 (1993); D. Chang, W.-Y. Keung, and I. Phillips, Phys. Rev. **D48**, 3225 (1993); and references therein.

[7] B. Grzadkowski Phys. Lett. **B 338**, 71 (1994).

[8] D. Chang, W.-F. Chang, W.-Y. Keung, hep-ph/9910465, Phys. Lett. **B478**, 239 (2000).

[9] S.Y. Choi and J. S. Lee, hep-ph/9907496 (1999); E. Asakawa, S. Y. Choi, J. S. Lee, hep-ph/0005118 (2000).

[10] D. Atwood, A. Soni, Phys. Rev. D**52**, 6271 (1995). Additional CP–odd observables in collider physics have been studied by J.F. Donoghue and G. Valencia, Phys. Rev. Lett. **58**, 451 (1987); W. Bernreuther and O. Nachtmann, Phys. Rev. Lett. **63**, 2787 (1989); G. Valencia and A. Soni, Phys. Lett. **B263**, 517 (1991); A. Bilal, E. Massó, and A. De Rújula, Nucl. Phys. **355**, 549 (1991).

[11] C.R. Schmidt and M. E. Peskin, Phys. Rev. Lett. **69**, 410 (1992).

[12] G. Kane, G.A. Ladinsky, and C.–P. Yuan, Phys. Rev. **D45**, 124 (1991).

[13] R.E. Cutkosky, J. Math. Phys. **1**, 429 (1960).

[14] LEP joint SUSY working group (LEPSUSYWG) for ALEPH, DELPHI, L3 and OPAL experiments,
note LEPSUSYWG/00-02.1 (http://lepsusy.web.cern.ch/lepsusy/).

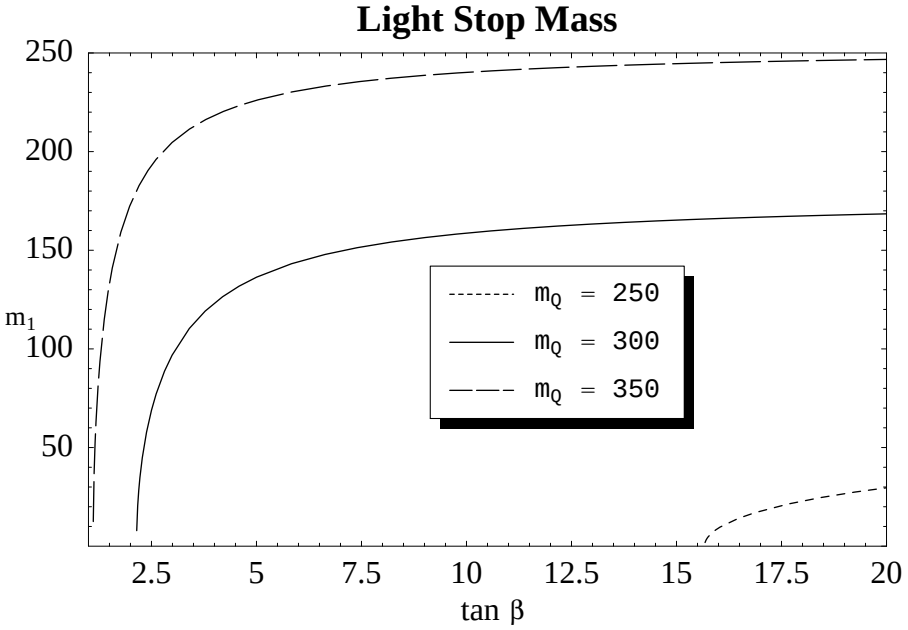

Fig. 4 Light stop mass m_1 in GeV versus $\tan\beta$ for the case $m_Q = m_U = 250, 300, 350\,\text{GeV}$, $\mu = 500\,\text{GeV}$, $A_t = 500e^{\frac{i\pi}{4}}\,\text{GeV}$.

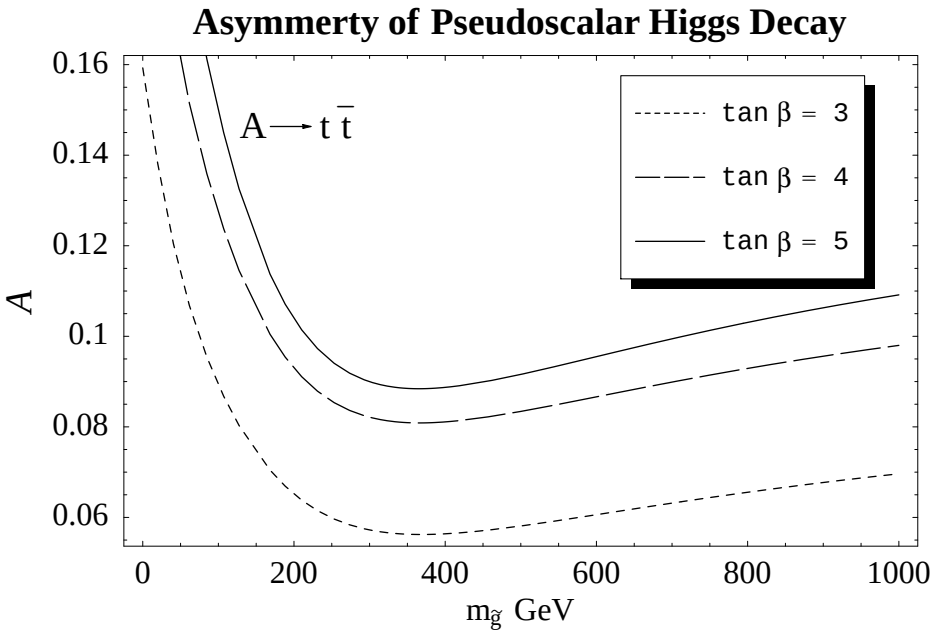

Fig. 5 Asymmetry of pseudoscalar Higgs decay, $m_Q = 300\,\text{Gev}$, $m_U = 300\,\text{GeV}$, $\mu = 500\,\text{GeV}$, $A_t = 500e^{\frac{i\pi}{4}}\,\text{GeV}$, $m_A = 400\,\text{GeV}$, $m_H = 420\,\text{GeV}$.

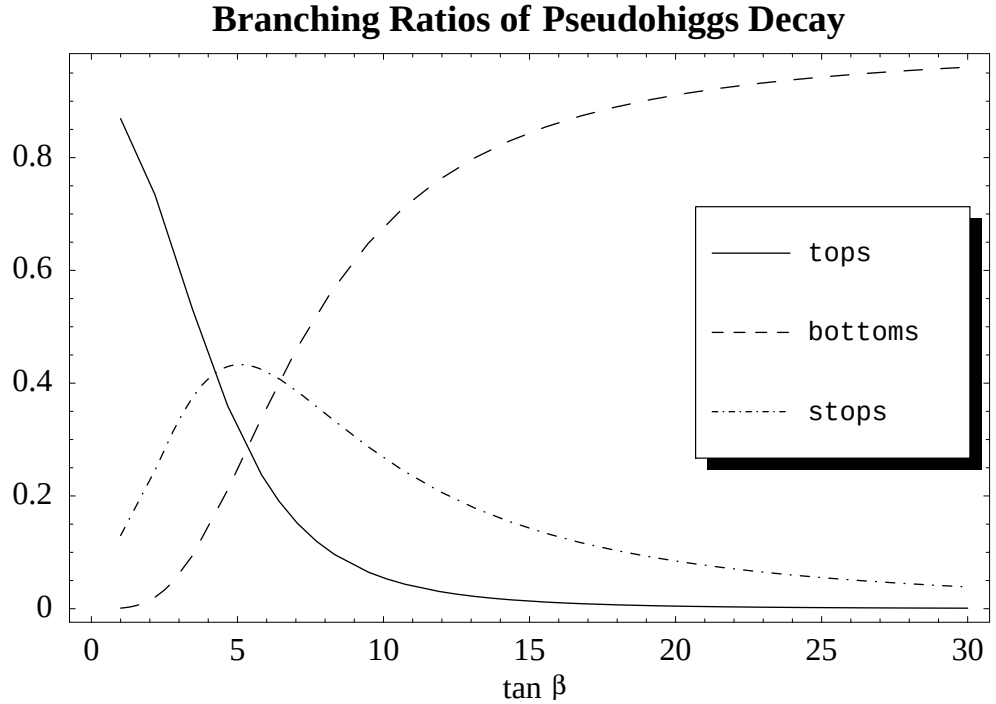

Fig. 6 Branching ratios for pseudoscalar Higgs decay, $m_Q = 300\,\text{Gev}$, $m_U = 300\,\text{GeV}$, $\mu = 500\,\text{GeV}$, $A_t = 500e^{\frac{i\pi}{4}}\,\text{GeV}$, $m_A = 400\,\text{GeV}$, $m_H = 420\,\text{GeV}$.

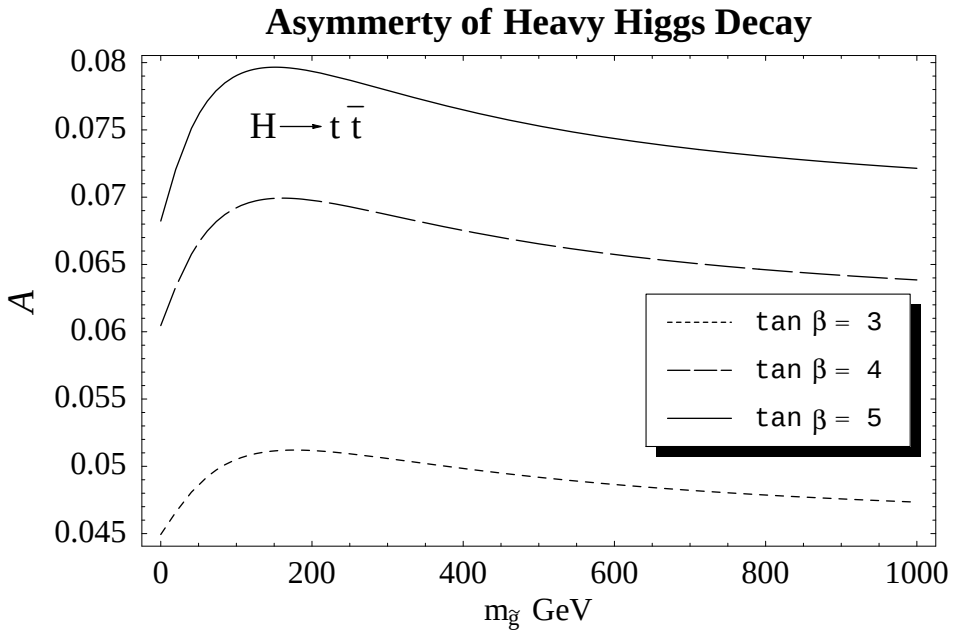

Fig. 7 Asymmetry of heavy Higgs decay, $m_Q = 300\,\mathrm{Gev}$, $m_U = 300\,\mathrm{GeV}$, $\mu = 500\,\mathrm{GeV}$, $A_t = 500e^{\frac{i\pi}{4}}\,\mathrm{GeV}$, $m_A = 400\,\mathrm{GeV}$,$m_H = 420\,\mathrm{GeV}$.

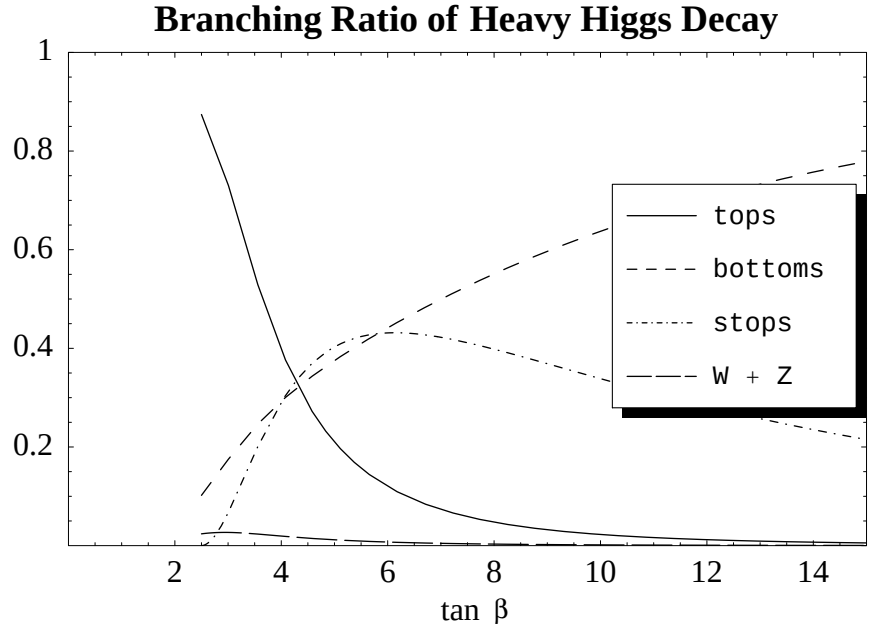

Fig. 8 Branching ratios for heavy Higgs decay, $m_Q = 300\,\mathrm{Gev}$, $m_U = 300\,\mathrm{GeV}$, $\mu = 500\,\mathrm{GeV}$, $A_t = 500e^{\frac{i\pi}{4}}\,\mathrm{GeV}$, $m_A = 400\,\mathrm{GeV}$, $m_H = 420\,\mathrm{GeV}$.